REVISION I

Crystal structure of lead uranyl carbonate mineral widenmannite: Precession electron-diffraction and synchrotron powder-diffraction study

JAKUB PLÁŠIL[1]*, LUKÁŠ PALATINUS[1], JAN ROHLÍČEK[1], LENKA HOUDKOVÁ[2], MARIANA KLEMENTOVÁ[1,3], VIKTOR GOLIÁŠ[4] AND PAVEL ŠKÁCHA[4,5]

[1] Institute of Physics ASCR, v.v.i., Na Slovance 2, 18221, Praha 8, Czech Republic; *email: plasil@fzu.cz
[2] Olbramovice – Městečko 16, 25752 Olbramovice, Czech Republic
[3] Institute of Inorganic Chemistry ASCR, v.v.i., Husinec – Řež 1001, 250 68 Řež, Czech Republic
[4] Institute of Geochemistry, Mineralogy and Mineral Resources, Faculty of Science, Charles University in Prague, Albertov 6, 128 43 Praha 2, Czech Republic
[5] Mining Museum Příbram, nám. Hynka Kličky 293, Příbram VI, 261 01

ABSTRACT

The crystal structure of the lead uranyl-carbonate mineral widenmannite has been solved from precession electron-diffraction data and refined using both electron-diffraction data and synchrotron powder-diffraction data. Widenmannite is orthorhombic, *Pmmn*, with a = 4.9744(9), b = 9.3816(16), c = 8.9539(15) Å, V = 417.86(12) Å^3. The structure was solved by charge-flipping and refined to an R_1 = 0.1911 on the basis of 301 unique, observed reflections from electron data, and to R_p of 0.0253 and R_F of 0.0164 from powder data. The idealized structure formula of widenmannite is $Pb_2(OH)_2[(UO_2)(CO_3)_2]$, Z = 2. However, both datasets suggest that the widenmmanite structure is not that simple. There are two symmetrically independent, partly occupied U sites. The substitution mechanism can be written as $U(1)O_2$ + $Pb(OH)_2 \leftrightarrow U(2)O_2$. When the U(2) site is occupied, the $U(1)O_2$ group is absent, the two OH groups are substituted by O^{2-} and one Pb^{2+}-vacancy. The chemical formula of the real structure should be written as $Pb_{2-2x}(OH)_{2-2x}O_{2x}[(UO_2)(CO_3)_2]$, where x is the probability of the substitution U(2) → U(1). The probability of occurrence of U(2) refines to x = 0.074(15) from the powder-diffraction data and to x = 0.176(4) from the electron-diffraction data. There

is one Pb site (nearly fully occupied), which is coordinated by eleven anions (up to the distance of 3.5 Å), including O and OH^-. The shorter Pb-O bonds form a sheet structure, which is linked by the weaker bonds to the uranyl-carbonate chains to form a three-dimensional framework structure.

Keywords: widenmannite, uranyl bicarbonate, crystal structure, precession electron diffraction, synchrotron powder diffraction

INTRODUCTION

Widenmannite is one of twenty-nine uranyl carbonates known from Nature as secondary alteration products of uraninite, typically formed in old open-mining adits of uranium mines (Krivovichev and Plášil 2013). Dissolution of naturally occurring UO_{2+x} (x = 0–0.67) – uraninite under oxidizing conditions maintains a high concentration of U^{6+} (as uranyl ion UO_2^{2+}) in percolating groundwater (Buck et al. 1994; Morris et al. 1996). The U^{6+} phases are also important alteration products of UO_2 in spent nuclear fuel (Forsyth and Werme 1992; Wronkiewicz et al. 1996). A good knowledge of the structural and thermodynamic stabilities of uranyl carbonates is particularly germane to the environmental chemistry of uranium (Clark et al. 1995; Finch 1997; Neu et al. 1997) due to the potentially high mobility of U in carbonate-bearing groundwaters (Langmuir 1978; Grenthe et al. 1994).

Widenmannite was first described from the Michael mine in Weiler, Schwarzwald, Germany, by Walenta (1976), as orthorhombic $Pb_2(UO_2)(CO_3)_3$, with a = 8.99, b = 9.36, c = 4.95 (Å) and V = 417 (Å^3), Z = 2 with possible space-groups $Pnmm$, $Pnm2_1$ or $P22_12_1$. Further occurrences worldwide were reviewed recently by Plášil et al. (2010), focusing on widenmannite and its occurrence at the Březové Hory deposit, Příbram ore district (Czech Republic). At this locality, widenmannite was found with other uranyl minerals at the Jánská

vein, where isotopic dating of widenmannite showed the presence of two generations related to different alteration processes.

To date, all attempts to solve the crystal structure of widenmannite have been unsuccessful, as widenmannite forms fine-grained poorly crystalline aggregates that yield x-ray powder diffraction patterns of insufficient quality for *ab initio* structure solution. This study presents the solution of the crystal structure of widenmannite from precession electron-diffraction (PED) and high-resolution synchrotron powder-diffraction data, showing that widenmannite is a uranyl bicarbonate with an OH group in the structure, rather than a tricarbonate as reported in all previous studies.

EXPERIMENTAL METHODS

Two widenmannite samples were used in this study; the labeling is the same as in the study of Plášil et al. (2010). Widenmannite I was used for the powder-diffraction work and consists of a mixture of widenmannite and kasolite. Widenmannite II was used for TEM study and contains yellowish globular aggregates of platy, prismatic crystals.

No crystals were of sufficient quality to give measurable X-ray diffraction patterns and therefore electron-diffraction study was carried out. A few aggregates of widenmannite II were dispersed in ethanol, and the suspension was then transferred to a carbon-coated copper grid . The sample was then examined in a transmission electron microscope Philips CM 120 equipped with a CCD camera Olympus SIS Veleta (dynamic range 14 bits) and a precession diffraction device (Digistar, NanoMegas). Accelerating voltage was 120 kV, corresponding to the electron wavelength, $\lambda = 0.0335$ Å. A crystal was left in an arbitrary orientation and a series of non-oriented diffraction patterns was recorded at a tilt angle ranging from -60° to +56° in steps of 1°, resulting in 117 diffraction patterns. The data were processed by the programs PETS (Palatinus 2011) and Jana2006 (Petříček et al. 2006). The structure was solved from the precession data by the charge-flipping algorithm (Oszlányi and Sütő 2004; Oszlányi and Sütő 2008; Palatinus 2013) using the program Superflip (Palatinus and Chapuis 2007), and subsequently refined by the full-matrix least-squares method using Jana2006 (Petříček et al. 2006). The model converged to $R_1 = 0.1911$, $wR_2 = 0.1855$ (with GOF = 8.17) for 301 observed reflections with $I_{obs}>3\sigma(I)$. A summary of data collection, solution, and refinement is given in Table 1. Atom

coordinates and displacement parameters are listed in Table 2. The U(1) and Pb atoms were refined with anisotropic-displacement parameters, the rest of the atoms were treated with isotropic parameters. The bond-valence analysis (Table 5) and charge-balance requirements suggested the O(6) atom is an OH group. Therefore we introduced the H atom into the model, even if it could not be located in the difference-Fourier maps. The H atom was treated with geometrical constraints to be kept in a tetrahedral arrangement with respect to the three Pb atoms linked to the O(6) site. The model obtained from PED was subsequently used as a starting model for Rietveld refinement (the H atom was not used in the refinement).

The synchrotron powder-diffraction data of widenmannite (sample widenmannite I) were collected at the Rossendorf beamline BM-20 at ESRF in Grenoble. The energy of the beam was set to 30 keV (λ = 0.41328 Å) to minimize absorption effects. The accurate wavelength was calibrated against the powder pattern of a standard (LaB_6). The beamline optics consists of a double-crystal Si(111) monochromator and two collimating/focusing mirrors (Si and Pt-coating). The crushed sample was placed into a 0.3-diameter mm borosilicate glass capillary rotated around its axis during data-collection. The diffraction pattern was collected at ambient conditions with a scintillation counter over the range 3–25° 2θ with a step-size of 0.0088°. The measured powder pattern contains peak positions of widenmannite and also of minor admixed kasolite. The Bragg positions of the diffractions are frequently overlapped in the pattern. For that reason, the kasolite (structure model from Fejfarová et al. 2013) was included as a second phase in the Rietveld refinement and its atom positions and ADP parameters were fixed during all refinement cycles. The structure model of widenmanite obtained from electron-diffraction data was used as a starting model for Rietveld refinement in JANA2006. To avoid unreasonable deformations of the hexagonal bipyramid and of the $(CO_3)^{2-}$ anions, oxygen and carbon atoms had to be constrained by soft bond-lengths and angle constraints. The position of the partly occupied U(2) site was confirmed by the presence of a large maximum in the difference-Fourier map. At the final stages of the refinement atom coordinates of all atoms were refined together with the isotropic ADP of heavy atoms and occupancy parameters of partly occupied sites, and also together with the profile parameters (unit cell, background and profile parameters, zero shift of the diffractometer, March-Dollase parameter, $MD_{(1\,0\,0)}$= 1.05, and phase fraction parameter, the amount of kasolite in the sample was approx. 7%). Isotropic ADP parameters of oxygen and carbon atoms were fixed at 0.038. The final agreement indices are R_p = 0.0246, wR_p = 0.0317, GOF = 2.17 (Table 1). The refined atom coordinates and displacement parameters and bond-valence sums are given in Table 3. Selected interatomic distances are listed in Table 4 (based on powder dataset) and are also included as a part of the CIF files deposited as supplementary files. The bond-valence analysis was done

following the procedure of Brown (2002) and is given in Table 5.

RESULTS

Idealized and real structure

The structure of widenmannite is a 3D framework (Fig. 1) consisting of uranyl carbonate chains interconnected by the network of Pb-O bonds. The idealized structure of widenmannite (Fig. 2a) contains one symmetrically independent U site, one Pb site, and has a sum formula $Pb_2(OH)_2[(UO_2)(CO_3)_2]$, $Z = 2$. However, both the powder- and electron-diffraction data indicated that both the U and Pb sites have low occupancies, and that there is a partly occupied U(2) site (Figs. 1, 2b). The U(2) site has an environment similar to that of U(1). To maintain charge balance, the low occupancies of U(1), U(2) and Pb must be accompanied by the low occupancies of the coordinated O sites. The only model that is compatible with charge neutrality and with the data seems to involve the substitution $U(1)O_2 + Pb(OH)_2 \leftrightarrow U(2)O_2$, *i.e.* the occurrence of the U at the U(2) site is accompanied by a vacancy at the U(1) site (i.e. no $U(1)O_2$ group), substitution of two $(OH)^-$ groups by O^{2-} and a vacancy at the Pb site. Moreover, the electron-diffraction data strongly indicate that the atom at the U(2) site is not localized in the plane of the CO_3 groups. To avoid unphysical features in the model, we decided not to include the splitting of the U(2) site. The substitution mechanism is illustrated in Fig 2b. The occupancies of the U(1), O(3), U(2) and Pb sites were constrained to maintain charge neutrality. The chemical formula of the widenmannite should thus be written as $Pb_{2-2x}(OH)_{2-2x}O_{2x}[(UO_2)(CO_3)_2]$, where x is the probability of the substitution U(2) → U(1). The probability of occurrence of U(2) refines to $x = 0.074(15)$ from the powder-diffraction data and to $x = 0.176(4)$ from the electron-diffraction data. These two values are not equal within three *e.s.d.s*, but they are not radically different. It is generally difficult to reliably refine atom occupancies from electron-diffraction data. For this

reason and because the powder is more representative of the bulk material, we believe that the Rietveld refinement gives a better estimate of the site-occupancies.

U and C coordination

The U(1) and U(2) cations are strongly bonded to two O atoms, O3 and O6, respectively, with the bond lengths characteristic for UO_2^{2+}; ~1.8 Å (Table 4). Each U atom is further coordinated by six O atoms, arranged at the equatorial vertices of hexagonal bipyramids capped by uranyl O atoms. The lengths of the equatorial bonds in U(2) coordination polyhedra are slightly longer (average ~2.6 Å; Table 4) than expected for hexagonal U coordination; ~2.45 Å (Burns et al. 1997). However, the geometry of the U(2) coordination is not entirely reliable due to the partial occupancy of the central cation of the U(2) polyhedron. The structure contains two independent C sites each coordinated by three O atoms forming planar CO_3^{2-} groups.

Pb coordination

There is one unique Pb site, nearly fully occupied by Pb^{2+} cation, which is coordinated by eleven ligands up to 3.5 Å (Table 4), including O and OH^- (Table 5). The asymmetry of the coordination polyhedron suggests that Pb^{2+} is lone-pair stereoactive in this structure. The Pb^{2+} cations are interconnected through Pb-O bonds into ribbons parallel to [010] (Fig. 3a), arranged in sheets parallel to (001) planes (Fig. 3b). Similar ribbons of atoms with lone-pair stereoactive electrons are known e.g. in laurionite (Smith 1899; Venetopoulos and Rentzeperis 1975; Merlino et al. 1993), containing Pb^{2+} cations, and medenbachite (Krause et al. 1996), neustadtälite and cobaltneustädtelite (Krause et al. 2002), containing Bi^{3+}.

Structural connectivity

In the idealized structure, the $U(1)O_2(CO_3)_3$ groups corner-share to form ribbons along [100], each pair of neighboring $U(1)O_8$ bipyramids sharing one CO_3 group (Fig. 4a). In the real structure, these chains are occasionally interrupted by a vacancy at the U(1) site. Instead, one U(2) site is occupied, forming a $U(2)O_2(CO_3)_3$ group that bridges two neighboring $U(1)O_2(CO_3)_3$ ribbons (Fig 2b). The interstitial linkage is provided by Pb^{2+}–O bonds, which link the U-bearing sheets in a zig-zag fashion (Figs. 1, 2a).

DISCUSSION

According to the structure solution, the idealized formula of widenmannite is $Pb_2(OH)_2[(UO_2)(CO_3)_2]$, $Z = 2$, in contrast to previous descriptions of widenmannite. The presence of OH^- groups in the structure was indicated by the Raman and infrared spectroscopic study of Plášil et al. (2010), who inferred substitution of two possible OH^- groups for one CO_3 group, but the details of the mechanism remained unclear.

Topology of the structure

The structure of widenmannite is unique among the uranyl carbonates and U^{6+} compounds in general. The structure has corner sharing of UO_8 hexagonal bipyramids, forming infinite chains along [100]. One CO_3 group is bidentately linked to two adjacent bipyramids, while the second CO_3 group is staggered at the opposite edge of each bipyramid (Fig. 4a). Adjacent UO_8^{∞} chains are occasionally interrupted by a vacancy, and linked through a $(U2)O_8$ bipyramid which is attached to the chains by corner sharing of equatorial O(2) and O(4) atoms and edge sharing with CO_3 groups. The idealized structure has the U(2) site vacant and the U(1) site fully occupied. This ideal structure has no relation with any other known uranium carbonate. If only the atom sites are considered regardless of their occupancy, the widenmannite topology is still unique, but can be related to the topology of

188 rutherfordine (Fig. 4c), which has neutral sheets of the composition $[(UO_2)(CO_3)]$ (Finch et
189 al. 1999). It is apparent that the widenmannite topology can be derived from that of
190 rutherfordine by a relative shift of every second row in the graph (Figs. 4b and d).
191
192 *The complementarity of the powder- and electron-diffraction data*
193 The present work is a notable example of how precession electron-diffraction
194 tomography and powder-diffraction (PD) are complementary techniques. It was not possible
195 to solve the structure of widenmannite from the PD data alone, whereas it was quite
196 straightforward to do so from ED, since it is going about single-crystal diffraction technique
197 and the positions of the light atoms can be better located in Fourier maps from the ED data.
198 However, the lattice parameters can be determined much more accurately from PD than ED
199 data. Moreover, the multiple diffraction inherent in the ED data makes least-squares
200 refinement difficult, and Rietveld refinement of the PD data gives much better figures of
201 merit and, more importantly, probably more accurate and more precise structure parameters.
202 This is particularly the case for the refinement of site occupancies. Nevertheless, comparing
203 the two refinements, we see that the largest distance between corresponding sites is 0.27 Å
204 for the partly occupied U(2) site, and all other distances are shorter than 0.15 Å. The average
205 discrepancy of distances (excluding the U(2) site) is 0.065 Å. This level of reliability is
206 sufficiently good to draw conclusions about the topology and bonding in the structure and
207 make approximate bond-valence analysis (Tables 2 and 3).
208
209 *The significance of widenmannite during alteration of uraninite*
210 Widenmannite is one of the supergene minerals that concentrate radiogenic Pb, similar
211 to e.g. kasolite or the Pb^{2+}-containing uranyl oxides hydroxy-hydrates (e.g. fourmarierite,
212 masuyite, richetite, etc.) (Finch and Murakami 1999). However, isotopic work by Plášil et al.

(2010) on widenmannite from the complex uranium-base metal hydrothermal vein indicated that the part of radiogenic Pb in both types of widenmannite (see sample description or the paper for details) is very low, ~1–2% only. Possibly, this is due to the prevalence of galena in the vein and thus non-radiogenic Pb prevails in the system. In localities where galena is lacking, widenmannite may concentrate radiogenic Pb in the structure.

A very good idea regarding the stability of widenmannite during continuous alteration processes provided us also the above mentioned study of widenmannite from Příbram (Plášil et al. 2010). This widenmannite occurrence, represented by "widenmannite I", constitutes an old *in-situ*, weathering association; it is a mixture of powdery widenmannite and kasolite in strongly weathered parts of the vein located ~30 m under the present surface, without any evidence for currently percolating water in the vein. This type of widenmannite was dated to more than 220,000 years based on the disequilibrium in $^{230}Th/^{234}U$ series. We point out that very similar samples of widenmannite were found on the old mine-dumps (see Plášil et al. 2005). These dumps are relatively treeless and have remained exposed to weathering for about 150 years. Widenmannite on these specimens has a relatively fresh appearance. It is associated with kasolite, a parsonsite-like mineral, and poorly crystalline U–oxide hydroxy-hydrates, forming massive aggregates ("gummites"). The powder x-ray diffraction patterns of the widenmannite samples from the dump did not suggest any significant decrease in crystallinity (or partial dissolution). The occurrence of apparently fresh well-crystalline widenmannite on the dumps indicates that the mineral is relatively stable when exposed to non-acidic or only weakly acidic conditions.

ACKNOWLEDGEMENTS

This paper fundamentally benefited from the thorough constructive review of Frank Hawthorne. The authors are also indebted to Sergey Krivovichev (St. Petersburg State University, St. Petersburg) for fruitful discussions on the widenmannite structure and for his review of the paper. We thank Peter Burns for his careful editorial

handling. Karla Fejfarová is acknowledged for her cooperation with the attempted single-crystal X-ray study. We acknowledged the European Synchrotron Radiation Facility for allocating the beamtime for the project CH-3085 and we to thank to Carsten Baehtz (Rossendorf beamline, ESRF Grenoble) for his kind help during the synchrotron experiment. The authors also thank the grant of MSMT of the Czech Republic, INGO LA 10010. This research was funded by the grants Premium Academiae of the ASCR, the post-doctoral grant no. 13-31276P of the Grant Agency of the Czech Republic to JP and the Fellowship J. E. Purkyně of the ASCR to LP.

REFERENCES CITED

Allen, P.G., Bucher, J.J., Clark, D.L., Edelstein, N.M., Ekberg, S.A., Gohdes, J.W., Hudson, E.A., Kaltsoyannis, N., Lukens, W.W., Peu, M.P., Palmer, P.D., Reich, T., Shuh, D.K., Tait, C.D., and Zwick, B.D. (1995) Multinuclear NMR, Raman, EXAFS, and X-ray Diffraction Studies of Uranyl Carbonate Complexes in Near-Neutral Aqueous Solution. X-ray Structure of $[C(NH_2)_3]_6[(UO_2)_3(CO_3)]_6 \cdot 6.5H_2O$. Inorganic Chemistry, 34, 4797–4807.

Brese, N.E., and O'Keeffe, M. (1991) Bond-valence parameters for solids. Acta Crystallographica, B47, 192-197.

Brown, I.D. (2002) The Chemical Bond in Inorganic Chemistry. The Bond Valence Model. Oxford University Press, Oxford, U.K.

Brown, I.D., and Altermatt, D. (1985) Bond-valence parameters obtained from a systematic analysis of the inorganic crystal structure database. Acta Crystallographica, B41, 244-248.

Buck, E.C. , Brown, N.R, and Derz, N.L. (1994) Distribution of uranium-bearing phases in soils from Fernald. Material Research Society, Symposium Proceedings, 333, 437–444.

Burns, P.C. (1999) The crystal chemistry of uranium. Reviews in Mineralogy, 38, 23–90.

Burns, P.C. (2005) U^{6+} minerals and inorganic compounds: insights into an expanded structural hierarchy of crystal structures. Canadian Mineralogist, 43, 1839–1894.

Burns, P.C., Ewing, R.C., and Miller, M.L. (1997) Incorporation mechanisms of actinide elements into the structures of U^{6+} phases formed during the oxidation of spent nuclear fuel. Journal of Nuclear Materials, 245, 1–9.

Clark, D.L., Hobart, D.E, Neu, M.P. (1995) Actinide carbonate complexes and their importance in actinide environmental chemistry. Chemical Reviews, 95, 25–48.

Čejka, J. (1999) Infrared spectroscopy and thermal analysis of the uranyl minerals. Reviews in Mineralogy, 38, 521–622.

Čejka, J, and Urbanec, Z. (1988) Contribution to the hydrothermal origin of rutherfordine. UO_2CO_3. Časopis Národního Muzea, 157, l–10.

Fejfarová, K., Dušek, M., Plášil, J., Čejka, J., Sejkora, J., and Škoda, R. (2013) Reinvestigation of the crystal structure of kasolite, $Pb[(UO_2)(SiO_4)](H_2O)$, an important alteration product of uraninite, UO_{2+x}. Journal of Nuclear Materials, 434, 461-467.

Finch, R.J. (1997) Thermodynamic stabilities of U(VI) minerals: estimated and observed

relationships. *In*: Scientific Basis for Nuclear Waste Management XX (Gray, W.J. and Triay, I.M., Eds.). Material Research Society, Symposium Proceedings, 465, 1185–1192.

Finch, R.J., Cooper, M.A., Hawthorne, F.C., and Ewing, R.C. (1999) Refinement of the crystal structure of rutherfordine. Canadian Mineralogist, 37, 929–938.

Finch, R.J., Buck, E.C., Finn, P.A., and Bates, J.K. (1999) Oxidative Corrosion of Spent UO_2 Fuel in Vapor and Dripping Groundwater at 90°C. *In* Scientific Basis for Nuclear Waste Management XXII (Wronkiewicz, D.J. and Lee, J.H. eds.), 556, 431–438. Warrendale, Pennsylvania, Materials Research Society.

Finn, P.A., Hoh, J.C., Wolf, S.F., Slater, S.A., and, Bates, J.K. (1996) The release of uranium, plutonium, cerium, strontium, technetium, and iodine from spent fuel under unsaturated conditions. Radiochimica Acta, 74, 65–71.

Forsyth, R.S., and Werme, L.O. (1992) Spent fuel corrosion and dissolution. Journal of Nuclear Materials,190, 3–19.

Grenthe, I., Fuger, J., Lemire, R.J., Muller, A.B., Nguyen–Trung, C., and Wanner, H. (1994) Chemical Thermodynamics of Uranium. Elsevier, New York, N.Y.

Krause, W., Bernhardt, H. J., Gebert, W., Graetsch, H., Belendorf, K., Petitjean, K. (1996) Medenbachite, $Bi_2Fe(Cu,Fe)(O,OH)_2(OH)_2(AsO_4)_2$, a new mineral species: Its description and crystal structure. American Mineralogist, 81, 505–512.

Krause, W., Bernhardt, H. J., McCammon, C., Effenberger, H. (2002) Neustädtelite and cobaltneustädtelite, the Fe^{3+}- and Co^{2+}-analogues of medenbachite. American Mineralogist, 87, 726–738.

Krivovichev, S.V. and Brown, I.D. (2001) Are the compressive effects of encapsulation an artifact of the bond valence parameters?. Zeitschrift für Kristallographie, 216, 245–247.

Krivovichev, S.V. and Plášil, J. (2013) Mineralogy and crystallography of Uranium. *In* *Uranium, from Cradle to Grave* (Burns, P.C. and Sigmon, G.E., Eds.), Mineralogical Association of Canada Short Course 43, Winnipeg MB, May 2013, 15-119.

Langmuir, D. (1978) Uranium minerals-solution equilibria. Geochimica et Cosmochimica Acta, 42, 547–569.

Merlino, S., Pasero, M., Perchiazzi, N. (1993) Crystal structure of paralaurionite and its OD relationships with laurionite. Mineralogical Magazine, 57, 323–328.

Morris, D.E., Allen, P.G., Berg, J.M., Chisolm-Brause, C.J. , Condradson, S.D., Hess, N.J., Musgrave, J.A., and Tait, C.D. (1996) Speciation of uranium in Femald soils by molecular spectroscopic methods: characterization of untreated soils. Environmental Science and Technology, 30, 2322–2331.

Neu, M.P, Reilly, S.D, and Runde, W.H. (1997) Plutonium solubility and speciation to be applied to the separation of hydrothermal waste treatment effluent. *In*: Scientific Basis for Nuclear Waste Management XX (Gray, W. and Triay, I.R., Eds.). Material Research Society, Symposium Proceedings, 465, 759–765.

Ondruš, P., Skála, R., Veselovský, F., Sejkora, J., and Vitti, C. (2003) Čejkaite, the triclinic polymorph of $Na_4(UO_2)(CO_3)_3$ – a new mineral from Jáchymov, Czech Republic. American Mineralogist, 88, 688–693.

Oszlányi, G. & Sütő, A. (2004) *Ab initio* structure solution by charge flipping. Acta Cryst. A60, 134-141.

Oszlányi, G. & Sütö, A. (2008) The charge flipping algorithm. Acta Cryst. A64, 123-134.

Palatinus, L. (2013) The charge flipping algorithm in crystallography. Acta Cryst. B69, 1-16.

Palatinus, L. (2011) PETS – software for processing of electron diffraction data. Institute of Physics, Praha, Czech Republic.

Palatinus, L., and Chapuis, G. (2007) Superflip – a computer program for the solution of crystal structures by charge flipping in arbitrary dimensions. Journal of Applied Crystallography, 40, 451–456.

Petříček, V., Dušek, M., and Palatinus, L. (2006) Jana2006. The crystallographic computing system. Institute of Physics, Praha, Czech Republic.

Plášil, J., Sejkora, J., Škácha, P., Goliáš, V., and Hušák, M. (2005) Compreignacite, uranophane and uranopilite from the Jánská vein, Březové Hory, Příbram. Bulletin Mineralogicko - petrologického oddělení Národního Muzea (Praha), 13, 192–195 (in Czech).

Plášil, J., Čejka, J., Sejkora, J., Škácha, P., Goliáš, V., Jarka, P., Laufek, F., Jehlička, J., Němec, I., and Strnad, L. (2010) Widenmannite, a rare uranyl lead carbonate: occurrence, formation and characterization. Mineralogical Magazine, 74, 97–110.

Smith, G.F.H. (1899) On some lead minerals from Laurium, namely, laurionite, phosgenite, fiedlerite, and (new species) paralaurionite. Mineralogical Magazine, 12, 102–110.

Venetopoulos, C.C., and Rentzeperis, P.J. (1975) The crystal structure of laurionite, Pb(OH)Cl. Zeitschrift für Kristallographie, 141, 246–259.

Walenta, K. (1976) Widenmannit und Joliotit, zwei neue Uranylkarbonatmineralien aus dem Schwarzwald. Schweizerische Mineralogische und Petrographische Mitteilungen, 56, 167–185. (in German).

Wronkiewicz, D.J., Bates, J.K., Wolf, S.F., and Buck, E.C. (1996) Ten-year results from unsaturated drip tests with UO_2 at 90 ºC: implications for the corrosion of spent nuclear fuel. Journal of Nuclear Materials. 238, 78-95.

Figure captions

Figure 1. The crystal structure of widenmannite viewed along [100]. The U(1) polyhedra is dark grey, the U(2) polyhedra is light grey and transparent. Pb atoms are grey.

Figure 2. Substitution mechanism in the structure of widenmannite. A) Idealized structure of widenmannite. The Pb site is occupied, while the U(2) site is vacant. B) The real structure of widenmannite. One of the U(2) sites is occupied, accompanied by a vacant Pb site and U(1) vacancy. The red atoms represents the position of O(6) (O^{2-} or OH^-).

Figure 3. The linkage between Pb and O atoms in the structure of widenmannite. A) The sheet structure of the Pb (grey) and O (red) atoms (bond-length cutoff set to 3.0 Å) viewed along [001]. The characteristic Pb-O ribbon, Pb-O(6) bond pair, is displayed in two colored

bonds-sticks. B) The same sheets in projection along [100]. The uranyl-carbonate layers are located between the Pb-O sheets, connected by weaker Pb-O bonds (see Figure 1).

Figure 4. A) Idealized structure sheet in widenmannite and B) its graph representation. Partly occupied U(2) polyhedra are transparent. C) Structure sheet in rutherfordine and D) its graph representation.

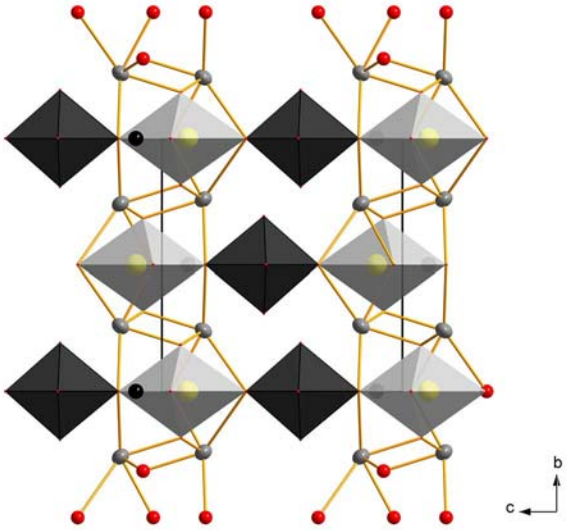
b
c

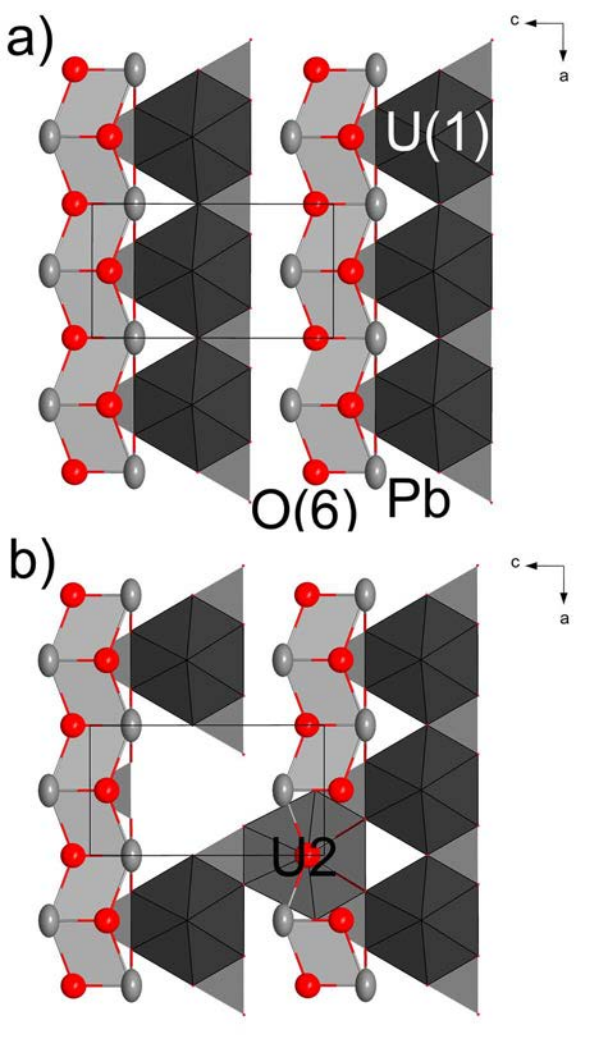
a)
c
a
U(1)
O(6)
Pb
b)
c
a
U2

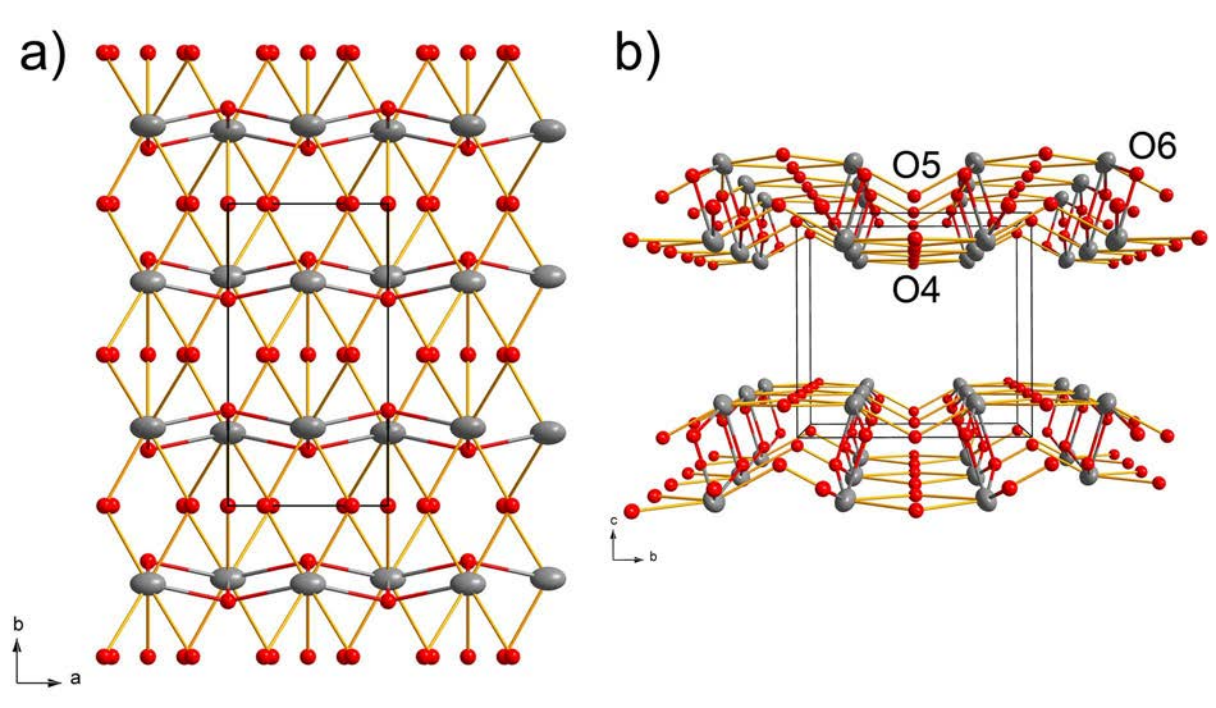
a)
b)
O5
O6
O4
b
a
c
b

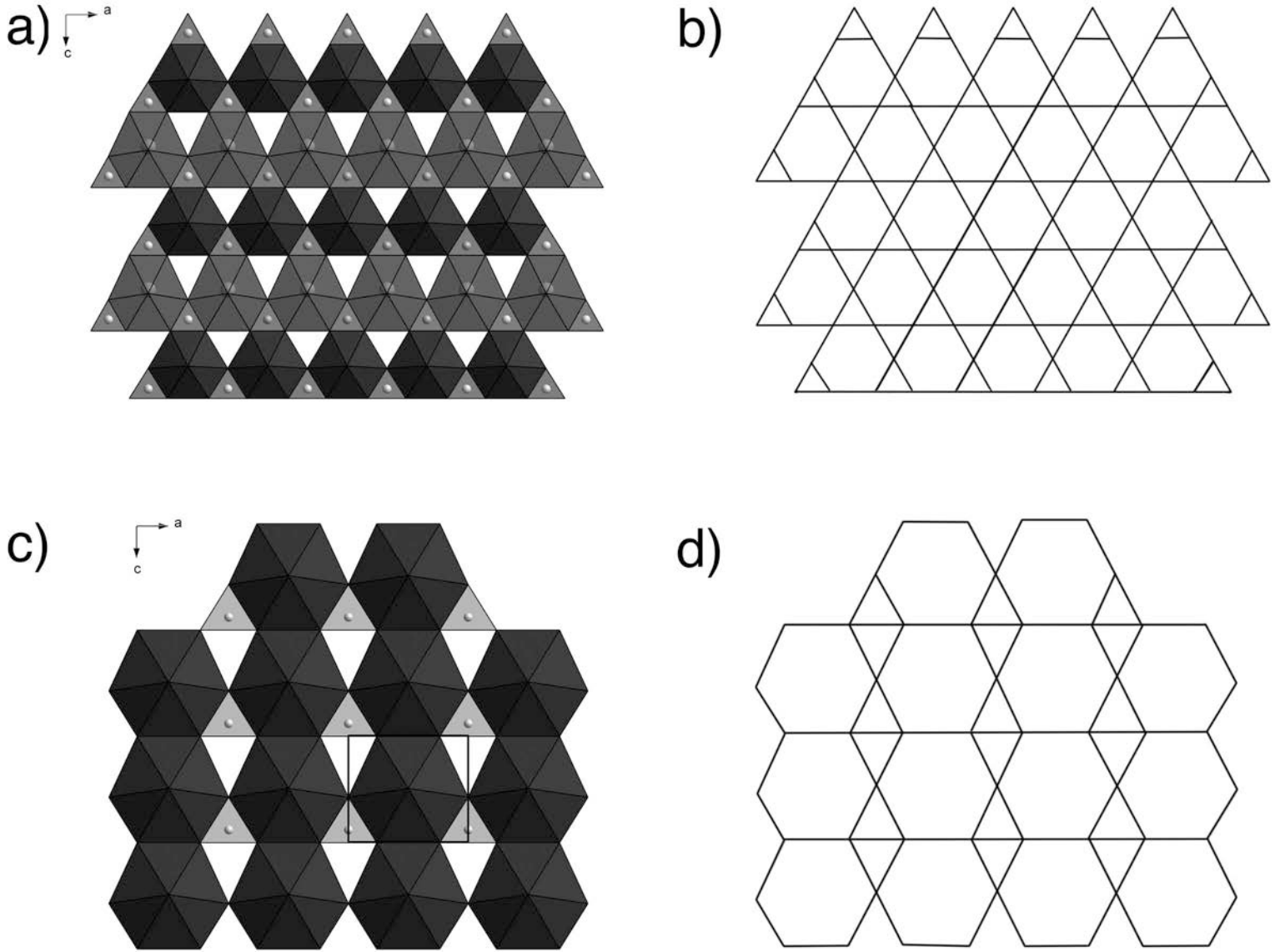
a)
a
c
b)
c)
a
c
d)

Table 1 Summary of data collection conditions and refinement parameters for widenmannite.

	PED		**Synchrotron powder diffraction**
a [Å]	4.9350(7)[#]	*a* [Å]	4.9770(7)
b [Å]	9.550(4)[#]	*b* [Å]	9.3869(13)
c [Å]	8.871(1)[#]	*c* [Å]	8.9597(12)
V [Å^3]	V = 418.08	*V* [Å^3]	418.59(10)
Z	2	Z	2
Space group	*Pmmn*	Space group	*Pmmn*
Data collection	*TEM Philips CM120*	*Data collection*	*Synchrotron, ESRF*
Temperature	293 K	Temperature	293 K
Source, wavelength	TEM, 0.0335 Å	Source, wavelength	ESRF BM20, 0.41293 Å
Crystal dimensions	770×600 nm	Specimen	Powder in 0.3 mm glass capillary
Collection mode	electron diffraction tomography	Collection mode	Rotation along φ axis
Limiting θ angles	0.1°–1.35°	Limiting θ angles	3.00–16.42°
Limiting Miller indices	–13<*h*<13, –11<*k*<11, –7<*l*<7	No. of points; observed reflections	1343; 98 [I_{obs}>3σ(*I*)]
No. of reflections	2688	Absorption correct. (mm^{-1}), type	9.40, cylindrical sample
No. of unique reflections	656	F_{000}	976
No. of observed reflections	301 [I_{obs}>3σ(*I*)]	*Refinement by Jana2006*	
Maximum sin(θ)/λ [Å^{-1}]	0.7	Param. ref., restraints, constraints	55, 15, 53
Data completeness	81.69% (all); 37.73% (obs)	R_p, wR_p, R_{exp}	0.0246, 0.0316, 0.0146
R_{int} (obs on F^2)	0.1692	GOF	2.17
Absorption correction (mm^{-1})		R_F, wR_F (widen)	0.0164, 0.0243
F_{000}	782	R_{Bragg}, wR_{Bragg} (widen)	0.0294, 0.0495
Refinement by Jana2006		R_F, wR_F (kasolite)	0.0278, 0.0291
Param. ref., restraints, constraints	35, 10, 6	R_{Bragg}, wR_{Bragg} (kasolite)	0.0479, 0.0577
R_1, wR_1	0.1911, 0.1855	$\Delta\rho_{min}$, $\Delta\rho_{max}$ (eÅ^{-3})	-0.42, 0.57
R_2, wR_2	0.3013, 0.1899	Weighting scheme	σ
GOFobs/all	8.17/5.49		
Weighting scheme, details	σ, $w = 1/(\sigma^2(F) + 0.0001F^2)$		

- The unit cell parameters obtained from PED are inherently less accurate, therefore in all refinements and subsequent calculations involving PED data the cell parameters obtained from synchrotron powder diffraction were used.

Table 2 Atom coordinates and displacement parameters for widenmannite (PED).

	x/a	*y/b*	*z/c*	U_{iso}	Occ.
U(1)	0.5	0.5	0.5786(4)	0.046(4)	0.824(4)
U(2)	0.5	0	0.923(4)	0.08(2)*	0.176(4)
Pb	0.5	0.7343(15)	0.1758(7)	0.140(6)	0.824(4)
C(1)	1	0.5	0.4161(16)	0.095(15)*	
C(2)	0.5	0.5	0.8957(15)	0.039(8)*	
O(1)	1	0.5	0.561(2)	0.067(10)*	
O(2)	0.775(3)	0.5	0.344(2)	0.058(7)*	
O(3)	0.5	0.683(4)	0.585(2)	0.033(6)*	0.824(4)
O(4)	0.278(3)	0.5	0.824(2)	0.074(8)*	
O(5)	0.5	0.5	1.038(2)	0.060(9)*	
O(6)	0.5	0.806(5)	−0.066(3)	0.093(9)*	
H(1)	0.5	0.887	-0.099	0.112	

	U^{11}	U^{22}	U^{33}	U^{12}	U^{13}	U^{23}
U(1)	0.0122(18)	0.113(10)	0.0142(19)	0	0	0
Pb	0.178(8)	0.169(16)	0.073(4)	0	0	0.00(6)

* refined with isotropic-displacement parameters.

Table 3 Atom coordinates and displacement parameters for widenmannite (powder diffraction).

	x/a	*y/b*	*z/c*	U_{iso}	Occ.
U(1)	0.5	0.5	0.5747(7)	0.012(4)*	0.926(15)
U(2)	0.5	0	0.893(11)	0.07(8)*	0.074(15)
Pb	0.5	0.7414(7)	0.1723(6)	0.056(4)	0.926(15)
C(1)	1	0.5	0.422(3)	0.002(14)*	
C(2)	0.5	0.5	0.891(3)	0.002(14)*	
O(1)	1	0.5	0.567(3)	0.002(14)*	
O(2)	0.775(4)	0.5	0.350(3)	0.002(14)*	
O(3)	0.5	0.692(2)	0.576(7)	0.002(14)*	0.926(15)
O(4)	0.272(4)	0.5	0.818(3)	0.002(14)*	
O(5)	0.5	0.5	1.036(4)	0.002(14)*	
O(6)	0.5	0.816(6)	−0.078(4)	0.002(14)*	
(H(1)	0.5	0.89479	-0.117295	0.0023*)#	

	U^{11}	U^{22}	U^{33}	U^{12}	U^{13}	U^{23}
Pb	0.087(10)	0.038(6)	0.044(6)	0	0	−0.008(5)

* refined with isotropic-displacement parameters. # not taken into account of further calculations

Table 4 Selected interatomic distances in the structure of widenmannite (powder data).

U(1)–O(1)	2.4895(11) (2×)	U(2)–O(2)	2.42(8) (2×)
U(1)–O(2)	2.43(3) (2×)	U(2)–O(4)	2.95(8) (2×)
U(1)–O(3)	1.802(19) (2×)	U(2)–O(5)	2.58(2) (2×)
U(1)–O(4)	2.46(3) (2×)	U(2)–O(6)	1.75(6) (2×)
<*U(1)–O_{Ur}*>	1.80	<*U(2)–O_{Ur}*>	1.75
<*U(1)–O_{eq}*>	2.46	<*U(2)–O_{eq}*>	2.65
C(1)–O(1)	1.30(4)	C(2)–O(5)	1.30(4)
C(1)–O(2)	1.29(3) (2×)	C(2)–O(4)	1.31(3) (2×)
<*C(1)–O*>	1.29	<*C(2)–O*>	1.31
	Pb–O(1)	3.37(2)	
	Pb–O(2)	3.089(17) (2×)	
	Pb–O(3)	3.42(4) (2×)	
	Pb–O(4)	2.781(11) (2×)	
	Pb–O(5)	2.574(18)	
	Pb–O(6)	2.35(4)	
	Pb–O(6)	2.683(16) (2×)	
	<*Pb–O*>	2.93	
O(1)–O(2)	2.24(3) (2×)	O(3)–O(4)	3.04(5) (2×)
O(1)–O(3)	3.074(11) (4×)	O(3)–O(6)	3.31(7)
O(1)–O(3)	3.16(3) (2×)	O(4)–O(4)	2.71(3)
O(1)–O(4)	2.62(3) (2×)	O(4)–O(4)	2.27(2)
O(2)–O(2)	2.74(3)	O(4)–O(5)	2.26(4)
O(2)–O(2)	2.24(3)	O(4)–O(6)	3.31(5) (2×)
O(2)–O(3)	3.04(5) (2×)	O(4)–O(6)	3.20(5) (2×)
O(2)–O(3)	3.17(2) (2×)	O(5)–O(6)	3.14(3) (2×)
O(2)–O(5)	3.13(4)	O(5)–O(6)	3.05(3) (4×)
O(2)–O(6)	3.19(5) (2×)	O(6)–O(6)	3.45(8)
O(3)–O(3)	3.04(4) (2×)	O(6)–O(6)	3.11(4) (2×)

Table 5 Bond-valence analysis of widenmannite structure (based on powder data).

Atom	U(1)	U(2)	Pb	C(1)	C(2)	∑*BV*
O(1)	0.41×2↓,$^{\times 0.926\rightarrow}$		0.06,$^{\times 0.926\rightarrow}$	1.30		1.68
O(2)	0.46×2↓,$^{\times 0.926\rightarrow}$	0.47×2↓,$^{\times 0.074\rightarrow}$	0.10×2↓,$^{\times 0.926\rightarrow}$	1.29×2↓		1.84
O(3)	1.61×2↓$^{\times 0.926\downarrow}$, $^{\times 0.926\rightarrow}$		0.05×2↓$^{\times 0.926\downarrow}$, $^{\times 0.926\rightarrow}$			1.54
O(4)	0.44×2↓,$^{\times 0.926\rightarrow}$	0.17×2↓,$^{\times 0.074\rightarrow}$	0.19×2↓,$^{\times 0.926\rightarrow}$		1.24	1.84
O(5)		0.35×2↓,$^{\times 0.074\rightarrow}$	0.29,$^{\times 0.926\rightarrow}$		1.28×2↓	1.72
O(6)		1.78×2↓,$^{\times 0.074\rightarrow}$	0.45$^{\times 0.926\rightarrow}$; 0.23×2↓,$^{\times 0.926\rightarrow}$			0.76
∑*BV*	5.60	5.54	1.93	3.88	3.80	

Values are expressed in valence units (*vu*). Site occupancies of the bonded atoms were taken into the calculations. ∑*BV*, bond-valence sums; ×↓→, multiplicity. U^{6+}–O bond strength (r_0 = 2.042, b = 0.506) from Burns et al. (1997); C^{4+}–O strength from Brown and Altermatt (1985), Pb^{2+}–O bond strength from Krivovichev and Brown (2001).